OriginalArticle

Neurological Tremor simulation using a skin tissue model and Tremor classification using Fiber Bragg grating sensors

Krishna Prasad S J[1*], Viswanath.T[2]

[1*]Dept. of ETE, Associate Professor M S Ramaiah Institute of Technology, Bangalore, India, krishnaprasad@msrit.edu;
[2]Dept. of ETE, Professor & Coordinator Centre for Imaging Technologies M S Ramaiah Institute of Technology, Bangalore, India. viswanath.talasila@msrit.edu

***Corresponding Author:** Krishna Prasad S J

*Dept. of ETE, Associate Professor M S Ramaiah Institute of Technology, Bangalore, India, krishnaprasad@msrit.edu;
DOI: 10.47750/pnr.2022.13.S08.496

Abstract

In the diagnosis of neurological disorders multiple sensing and analysis technologies have been developed. In this work effort is to synthesize tremor signals on modal and harmonic analysis workbench and classify the smokers and non-smokers tremor signals in the perspective of optical sensing. Associated objective is to analyse and extract performance parameters using the skin-tissue models of smokers and non-smokers classes in modal/harmonic analysis tool boxes and to inspect the force effects on Fiber Bragg grating sensor. The novelty lies in the fact that a biophysical computational model on deep layers of human skin is implemented on which tremor analysis have been carried out. Further the model is employed to inspect effects which are mechanical on Fibre Bragg grating sensors subjected to tremor motions indicating subtle changes in skin deformation. The developed models correlates tremor induced frequencies and disorders of neurology as the zones of frequencies deployed for synthesis are in the clinical tremor zones of frequencies.

Keywords— FBG sensors, CAD workbench, Tremors. Mass participation ratio, RSoft workbench.

I.INTRODUCTION

In Medicine disorders of neurology is affecting not only nerves found throughout the human body and spinal cord but also brain. Globally among races there is an upsurge of disorders connected to nervous systems. Tremor analysis is a part of that branch of medical research. Tremor in humans can be formally defined as involuntary rhythmic muscle relaxation and contraction based oscillations of one or more body joints due to neurological disorders. These movements are involuntary and are persistent affecting legs, hands, trunks and arms. A tremor can be a symptom of neurological disorders. There are various rating scales are used such as Fahn–Tolosa–Marin Tremor Rating Scale (TRS), essential tremor rating assessment scale (TETRAS) and Unified Parkinson's disease rating scale (UPDRS) used to assess tremors in PD patients. Tremor scales vary with reliability and validity. They are not sensitive enough to assess subtle changes over time [1,3,4]. There is a need of new innovative techniques to assess and model the tremors. In this study an interesting case of classification of tremors based on frequency of human skin has been realized. This study has focus of investigation of intensity of tremors on smoking and non-smoking classes through a skin model synthesized on ANSYS workbench. Further this model is used to inspect mechanical effects on a variant of optical sensor namely Fiber Bragg grating sensor. Optical sensing advantages of minimal noise, high sensitivity for subtle changes to quantify tremor has been explored in this study. The results of study which can be correlated to frequency of tremors which will be important finding for medical community to identify neurological disorders. Further experimental works will strengthen the findings of this study.

One of the cause of the tremors is the onset of neurological disorders others being extensive usage of Tobacco, drugs (including caffeine, corticosteroids), alcohol, mercury poisoning. Primary causes also include minimal sleep hours, deficiency of vitamins or enhanced stress levels. Possibilities of occurrence of tremor are at any age but quite common among older and mid-age persons. Tremor types may be triggered and become aggravated during times of strong emotion or stress or during certain postures or movements or when subjects are exhausted. Tremor classification is based on situations either stationary or action related. Action tremor is further bifurcated into postural and kinematic. This classification of tremors has correlations with disease studies, which has high relevance on therapeutic options. Tremor classification is also on the frequency, body parts and etiology [1,2].

Intentional motions such as pressing switch can cause cerebellar tremor of range 4-5Hz.Parkinsonian tremor usually at rest may also be evoked with actions it is oscillations of frequency 4-6Hz. Physiological tremor oscillations are at a frequencies 8–12 Hz which is usually present in healthy subjects. There may be enhanced physiological tremor due to tobacco and alcohol consumptions. Neurological disorders presence for certain duration leads to variations in stability of body leading to tremors. Among that tremors Essential tremor (ET) is one of the important tremor variety .ET is termed as mutually exclusive tremor in which group of symptoms which consistently occur together of upper limb of bilateral action tremor of minimum 3 years sustainment either with or without problems in other parts of body (lower limbs head or voice). Orthostatic tremor feature is (>12 Hz) systematic muscle shrinking occurring in the trunk and legs instantly after subject stands. Holmes tremor is a result of causes like radiations, toxoplasmosis, tumors, head injury, stroke effects, and blood vessels blockages and tranquilizers effects. Holmes tremor is featured by action tremor severity greater than that of the rest ones (frequencies <4.5Hz) [2,5]

Researchers have used sensors and sensing technologies for assessment of tremors. For a biomedical clinical instrument, it is a rule to place sensor at appropriate joint with minimal electrical interference to quantify tremor. Sensors should designed to suit comfort levels and should be of diagnostic standards. An issue of finding points of origin of tremor termed as localization is principal factor in tremor research. The type of sensor selected influences improvising and understanding responsiveness of supraspinal and spinal structures and how neuromuscular activity influence tremor. In one of the study various sensors accelerometers gyroscopes goniometers, optoelectronic devices, wearable orthosis and force sensors were compared and it has been concluded that works should be focussed towards choosing sensors of interest for a slated experiment in order to generate data in conformance with functional clinical measurements of severity of tremor. Deviations are predicted, but have to be minimal as possible. Assessment techniques which are sensitive are required. Clinically-validated sensors miniature in size, light weight configurability and lesser in noise have high predictability to become successful [6].

There are also wearable sensors through which certain motor function disabled patients analysis has been done provisioning titration of medical in nature in patients with Parkinson's disease and measuring motor recovery actions in survivors of stroke but are in process of rehabilitation. As per the study a robust wireless sensor network is necessary to collect the data of patients remotely and to develop analysis technique to which renders clinical information relevant to sensor data which is miniature in nature [7].

Several of the works [8,9] has done analysis of postural and rest state of PD tremor with the help of accelerometer on wrist and hand under both stress and resting conditions. Also a fusion of data from various sensors namely magnetometers, gyroscope and accelerometer sensors has been done. From fusion orientation of body segments are estimated employing Kalman filter.

Bonato et al.[10] illustrated and implemented wearable sensors both in ambulatory and in-house subjects. To supplement the same patient data correlating with monitored events was designed and implemented. Fuzzy systems and neural networks were employed to predict critical events. Also this study mentions dynamically response intervention for tremor suppression. It focuses on efficacy of sensing and control technologies for suppression of tremor.

The literature outlined above requires the use of clinical subjects for the assessment of measurement, analysis and control efficacy. In general, this is difficult, as clinical studies require extensive preparation and meticulous planning. It would be of interest to the research community if there were a possibility to conduct a part of these studies through the use of advanced simulation tools. Here the idea is that much of the sensing and control algorithm development can be done on simulation platforms, and only the final system can be deployed and tested in clinical studies. This has the potential to hopefully allow researchers to design and test multiple technology platforms before going into actual clinical studies. One approach adopted in this paper is the use of ANSYS mechanical workbench in conjunction with RSOFT optical testbench to demonstrate development of new sensing techniques in the field of tremor measurements.

There are studies done using ANSYS work bench using human joint models and assessment of tremors and in addition there are certain studies executed by realizing FBG sensors on ANSYS workbench. Some of those are further discussed to develop ideas on the present study undertaken. One of the study implements model of finite element analysis (FE) of a hand-arm system of humans to derive mode shapes and natural frequencies. The FE model is compared with benchmark by comparing parameters of modes documented from vibrations obtained from experimentation with the framework of transmissibility and operational modal analysis (OMA). Modal and harmonic simulation of FE model is performed considering conditions at boundary for two cases. The first case focus is on fixed shoulder condition while the second case introduces the trunk permitting Shoulder motion. The results demonstrate that second model natural frequencies enabling motion of shoulder are correlating with those documented experimentally. Inferences are that the ANSYS can be used to measure natural frequencies and mode shapes of a human hand arm system. Also ANSYS analysis is the primitive step to synthesize biological signals and perform medical diagnostics on the same [11].

One of the study mainly introduces vibration sensor of Fiber Bragg grating (FBG) employed to interrogate the degree and orientation of critical parts and other parts. Structures of three varieties are visualized. The natural resonance

frequency of first order and image of cloud vibration are documented using ANSYS mechanical. This study quantifies cantilever beam structure strength and structure of single beam to have design optimization. Inferences are that the ANSYS can be used for modal analysis of the structure and is a software environment suitable for that type of analysis .Another observation of this study is that it has explored the implementation of functionality of FBG sensor in ANSYS environment [19].

One of the study presents a innovative mechanism of sensing employing only one inertial measurement unit (IMU) sensor system deployed at ankle, to quantify and estimate not only cycle of parameters in gait but also gait expenditure in energy. This realized work supports active techniques assistive in nature called as a exoskeleton and Electrical Stimulation functional ones in nature (FES) . Work infers that it has estimated the heal strike parameter of Gait cycle 10ms delay from actual value and it has conducted study on data collected from two volunteers. Here the type of sensor used has impact on the accuracy of technology developed. Also as this is an experimental work, there is a possibility of increasing the accuracy by incorporating sensors with higher sensitivity and less noise like Fiber Bragg grating sensors [20].

In a study it has been quoted that Fibre Bragg grating (FBG) sensors has become one of the most rapidly progressing sensing in optical fibre sensors. FBG sensors are currently emerging from the laboratory to find practical applications. Rapid progress has been made in both sensor system developments and applications in latest decade [13].

The small size and high elasticity enables design of fiber optic sensors (FOS) miniature in nature, electromagnetic interference resistance and electrical circuit connection absence , electromagnetic field of high values and safer than existent technologies (in terms of sensitivity and frequency drifts) enabled FOS sufficient for majority common applications in medicine. These features paved way and elevated the potent usage of FOS in medicine projecting them especially attractive for medicine applications. In the literatures it is highlighted that it enables Temperature and external vibrations termed as contributors to signal noise and drift were considered by proper system design.[14].

A LIMITATIONS OF WORK

Sensor such as accelerometers, gyroscopes, and wireless nodes based one, goniometers and sensors in wearable orthosis has several limitations highlighted as:

- Sensors selection is based on weight, size, sensitivity, frequencies and the S/N ratio.
- Sensor highlighted cannot be multiplexed easily and even it is multiplexed there are chances of overlapping of data
- Sensors highlighted are corrupted by noise. Placing sensors without restricting movements is challenging.
- Sensors used for diagnosis should be of diagnostic standards.
- Calibration of these sensors is necessary and challenging.
- Sensors to suit comforts, be artistic, affix firmly and compact to patients.

There are also Diagnostic methods limitations. It depends both on mood of patients and focus of doctor. Both Tremor recording and diagnostic methods have to be combined to get accurate assessment. Kinematic motor task and tremor frequencies will have to be assessed accurately in medical diagnostics.

B NOVELTY OF THE STUDY

For tremor assessment, various sensors have been deployed in the literature. Intensity along with the detection of the type of tremor based on the frequency domain analysis has been realized. It is challenging in this research to eliminate the acquisition noise of sensors. In this case study,effort is to synthesize tremor signals on ANSYS workbench and classify the smoker's and non-smokers' tremor signals from the perspective of optical sensing. The innovation lies in the fact that a biophysical computational model on deep layers of human skin is implemented on which tremor analysis have been carried out. Further the model is employed to inspect the effects which are mechanical on Fibre Bragg grating sensors subjected to tremor motions. The developed models correlate tremor-induced frequencies and disorders of neurology as the zones of frequencies deployed for synthesis are in the tremor zones of frequencies. In the diagnosis of neurological impairments, limited work is done using ANSYS a CAD tool, and RSoft workbench. Once the model is synthesized the directional deformation and stresses in each of the three directions are documented. One can analyze the reflected wavelength of sensors with minimal noise in tremor studies. This study provides both optimizations in diagnostics and solves ethical issues.

C BASE LITERATURE OF STUDY

A study demonstrates model of the human skin employing Finite element analysis (FE) to extract mode shapes and natural Frequencies. The FE model is benchmarked by parameters of modes got from vibration extracted experimentally by employing transmissibility and operational modal analysis (OMA). These measurements prove useful in different domains of interest listed from medicine, forensics and cosmetics. In this experimentation a micro robot sensitive to force exerted on three dimensional deformations to surface of skin in various areas of arms for around 20 volunteers has been employed. Force displacements of each area were quantified in three directions of application. It is observed that all areas exhibited anisotropic, non-linear and viscoelastic characteristics. All volunteers exhibited same qualitative features of anisotropy. It was observed that stiffest force displacement response was along longitudinal right forearm. The anterior left forearm response was hardest in 20 degree direction in longitudinal fashion of the forearm. On the

averaging end upper arm posterior response was less hard than the forearm response .It provides a basic framework to differentiate the left handers and right handers. Also response of forearm of hand and upper arm of hand can be different [18]

In a study conducted it was inferred tobacco smoking can be damaging factor to the skin. Tobacco smoking is also affecting biophysical parameters of the skin. It is in the areas of epidermis, dermis and nasolabial folds thickness and density in particular have variations. Objective of the study conducted was to compare and contrast biophysical properties of biophysical nature of human skins of smokers and non-smokers. The samples in that study are a group of 24 non-smokers and 28 current smokers. The trans epidermal water loss, erythema, melanin content, pH, sebum, elasticity parameters (R0, R2, R5) of skin, friction, epidermis, echo-density, dermis thickness , and hydration of the stratum corneum were measured on right cheek, middle forehead and right inner arm of volunteers. Additionally surface area, volume and depth of right nasolabial folds were documented. The mean of these statistics in non-smokers were compared with that of smokers by statistical test which is independent. Thickness of epidermis and dermis was not only higher in smokers in all measurements but also density of epidermis was lower in smokers. The differences were noticed on forehead was significant. Density of dermis was lower in smokers, but difference on arm was significant. Skin density for smokers at the forearm is indicated as 158 kg/m2 and that of non-smokers happens to be 168 kg/m2 as per their study enacted .These parametric values are employed in the new material created in the engineering material tab to differentiate between smokers and non-smokers in the Present study undertaken [12].

Considering all of the literatures, main setbacks noticed were the sensors are purely electronics in nature. Also there are variants in the sensors accelerometers, gyroscopes goniometers, optoelectronic devices; wearable orthosis, force sensors and even wireless nodes. Drawbacks of these sensors are that the sensors are not subtle to changes in low frequency tremor ranges as it is measured in time domain. Researchers also analyzed sensor outputs in the frequency domain. A mathematical conversion from time to frequency consumes time to arrive at results. Also time to frequency conversion will not be accurate .As these changes has an effect on analysis, and accuracy of the analysis with eventual predictions depends on the accuracy of sensors. All electronic sensors are affected by the acquisition noises and also power supply noises. In addition sizes of the sensors, adaptability of sensors for in vivo studies are also posing problems to deploy them to understand the neurological tremors [14]. Multiplexing sensors is complex and hence optical sensors have become popular. Considering the problems associated with the sensors highlighted optical sensors deployments are gaining popularity. Advantages of optical technology like multiplexing the sensors effortlessly and eventually visualize the outputs simultaneously; deployments in noise, electrical and nuclear hazardous environments are advantages, which made optical sensors to gain high popularity[13]. Researchers have employed various sensors for measuring tremors. For feasibility purposes popular are accelerometers. Bias, shot and random walk noises were quantified by Weiner filter in previous studies undertaken. When optical sensors are considered acquisition noises, bias, shot and random walk noises are minimal. Effort is not needed to estimate the noises and cancel the noises.

If one considers the base literatures for the study the inferences drawn happens to be that we can deploy ANSYS tool to enact the modal analysis to any structure proposed .One can implement on modal analysis and further get the inference of harmonic analysis in any of the three directions in the space of the material. Also in one of the literatures [18] It was observed that stiffest force displacement response was along longitudinal right forearm. The anterior left forearm response was hardest in 20 degree direction in longitudinal fashion of the forearm. On the averaging end upper arm posterior response was less hard than the forearm response .It provides a basic framework to differentiate the left handers and right handers. Also response of forearm of hand and upper arm of hand can be different. In another study [12] observations are that Density of dermis was lower in smokers, but difference on arm was significant. Skin density for smokers at the forearm is indicated as 158 kg/m2 and that of non-smokers happens to be 168 kg/m2 as per their study enacted .These parametric values are employed in the new material created in the engineering material tab to differentiate between smokers and non-smokers in the present study undertaken. In another study Inferences are that the ANSYS can be used for modal analysis of the structure and is a software environment suitable for that type of analysis .Another observation of study referenced is that it has explored the implementation of functionality of FBG sensor in ANSYS environment [19].

D WORK ORGANISATION

This work is organized as follows: Section 1 states Introduction, works undertaken prior to this study, innovation and limitations. Section 2 provides methods and materials to simulate human skin model in ANSYS mechanical environment, apply tremor frequencies and mathematically port the effect of tremors on Rsoft Grating mod environment to get effect of tremors on optical sensor FBG. Section 3 documents the results and analysis. Section4 provides conclusions and future directions.

II. METHODS AND MATERIALS

The methods professed are depicted in the flow diagram of Figure1. Five steps are visualized:

- In Step1 The frequencies of tremors due to neurological disorders are extracted from literatures. These are represented in Table1 [15][16].

- In Step2 The human skin model and skin layers are synthesized in ANSYS mechanical.
- In Step3 The modal and harmonic analysis of human skin of non-smokers and smokers classes were executed and deformations resulting from forces applied were also measured and captured from simulation runs. It is through ANSYS Workbench using FEM.
- In Step4 Deformation/tremor resulting from simulations runs for harmonic frequencies obtained are the inputs to Grating Mod tool where FBG sensors are synthesized. Further Bragg reflections on ranges of wavelengths were measured and recorded in addition to theoretical calculations.
- In Step5 The directional deformation of non-smokers and smokers population and reflected wavelength Resulting were simulated and analysed.

STEP 1 DETAILS: The Literature review analysis are documented in Table 1. Critical Observations are frequency variations. In this study variables indicated in the Table 1 were taken. Tremors considered were Parkinsonian with 3−7 Hz, Holmes with 4−5 Hz, Neuropathic with 4−7 Hz and Task specific with 5−7 Hz. Also physiological tremors can also be considered .In the simulations the applied forces were of frequencies ranging from 8Hz to 50 Hz. Frequencies were synthesized through modal analysis and harmonic analysis tool sets in ANSYS workbench. Harmonic analysis is carried out in same ranges of tremor frequencies due to presence of neurological disorder.
STEP 2 DETAILS: human skin model is synthesized in ANSYS.Skin areas considered are epidermis and dermis layers of the hand and wrist. The parametric dependency of the human skin is as detailed in the table 2 and table 3.
STEP 3 DETAILS: Forces of 100 N to 600N were applied. Suitable forces were natural choice depending on the Maximum deformation and tolerances in the models. These can be decided from simulation runs.
STEP 4 DETAILS: Deformation/tremor resulting from simulations runs for harmonic frequencies obtained are the inputs to Grating Mod tool where FBG sensors are synthesized. Further Bragg reflections on ranges of wavelengths were measured and recorded in addition to theoretical calculations.
STEP 5 DETAILS: The effects of force on human skin i.e changes in the reflected wavelengths were analysed for both smokers and non-smokers for various ranges of harmonic frequencies. Additionally stresses in the deeper layer were also recorded.

A SIMULATION STEPS IN ANSYS WORKBENCH

If one considers human body parts, one need to know about the deployment points of the FBG sensors. FBG sensors are being deployed on the surface layers of hands and wrist in the simulation study. They can also be deployed on the ankles if the parameters of the leg ankle joints are needed. The generated deformation values are applied to the FBG sensors affixed on the human forearm of the subject under test. The dielectric, electrical, Young's modulus, density properties of skin and its inner muscles were extracted from the literatures shown in Table 2and Table 3. Employing these properties skin models were developed for conducting simulation studies.
In the ANSYS 2022 a latest product release new tool set on optics are available for engineers. There is simulation flexibility in the tool for application areas ranging from industrial, Flow analysis and medical diagnostics in latest releases.

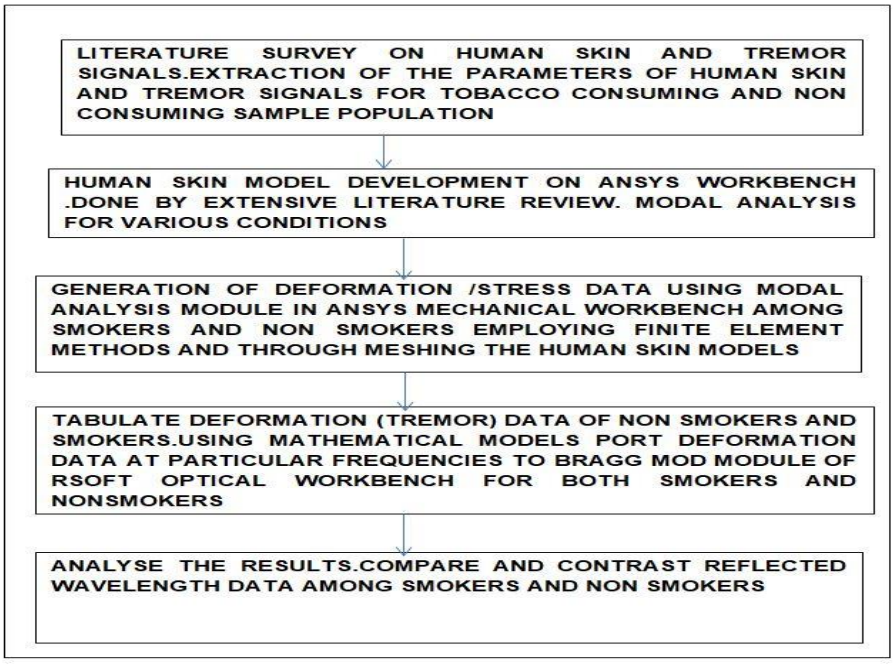

Figure1. Flow diagram of the simulation

Table 1. Tremor variants with frequencies[15]

TREMOR TYPE	PARKINSONIAN	PHYSIOLOGICAL	HOLMES	NEUROPATHIC	TASK SPECIFIC	ESSENTIAL
FREQUENCY	3-7 Hz	3-30HZ	4.5 HZ	4-7 HZ	5-7 HZ	4-12 HZ

Table 2 Electrical and Magnetic Properties of skin parts [17]

Tissue	Permittivity	Electrical Conductivity S/M	Density of skin Kg/m3	Heat capacity of the skin (J/kg/°C)	Thermal Conductivity (W/m/°C)	Heat Transfer rate (ml/min/kg)	Heat generation rate (W/kg)
Skin	7.29E+1	4.91E-1	1109	3391	0.37	106	1.65
Skull Cortical	1.53E+1	6.43E-2	1908	1313	0.32	10	0.15
Spinal Cord	4.73E+1	3.38E-1	1075	3630	0.51	160	2.48
Muscles	6.60E+1	7.08E-1	1090	3421	0.49	37	0.91

B SIMULATION MODAL AND HARMONIC ANALYSIS

The first step in the simulation is modal analysis. Briefly mathematics and requirement of modal analysis is dicussed. Further procedure for execution of modal analysis is discussed.

A MATHEMATICS OF MODAL ANALYSIS

Modal analysis is done to analyse resonant vibrations of physical systems. It also projects an idea on design response to loads dynamic in nature. It is a handy tool for control of solution for associated dynamic analysis.

For mathematics of modal analysis following equation 1 is considered for general equation of motion.

$$[M][\ddot{u}]+C[\dot{u}]+K[u]= \{F(t)\} \quad (1)$$

Where K is the stiffness coefficient, C is the damping ratio, M is the mass and F is the external applied force varying with time. Here ü is acceleration, ú is velocity and u is displacement.
Assuming vibrations free in nature and neglecting damping we get

$$[M][\ddot{u}]+K[u] = \{0\} \quad (2)$$

One needs to assume motion harmonic in nature and hence

$$u = U \sin(\omega t) \quad (3)$$

and we get

$$\{[K]- \omega 2[M]\}\{u\} = \{0\} \quad (4)$$

This is quadratic equation which has roots ωi (Eigen values) where i range from 1 to Degrees of freedom. Here the degrees of freedom are ranges of frequencies of vibration. Corresponding vectors are u the Eigen vectors. An Eigen value gives the principal components of entity decomposed in frequency domain
The Eigen values square roots are ωi, the natural circular frequencies of the structure. Frequencies which are natural termed as fi are then calculated as $fi=\omega i/ 2\pi$.It is the frequency fi which is natural vibration of structure whose ranges are decided by user and then respective outputs are recorded from modal analysis tool simulation runs .The Eigen vectors {u}i indicates the shapes of modes which are nothing but the shape aligned by structure vibrating at natural frequency fi.

B PROCEDURE OF SIMULATION EXECUTION IN ANSYS

The skin and its inner muscles electric and dielectric and properties were obtained from the literature database as depicted in Table 2and Table 3.These properties were incorporated for both smoking and non-smoking class of the population in the engineering materials tab in Modal analysis module working in ANSYS workbench. As observed the density of smokers is 158 kg/m2 and that of non-smokers is 168kg/m2[12].Accordingly these new materials have been

added to engineering resources of engineering materials tab. This is very important step to initialize the simulation study among smokers and non-smokers.

Table 3. Electrical and mechanical data values of human skin among non-smokers and smokers [12]

Sl. No	Parameter of Human skin	Parametric values
1.	Skin Density(Normal skin)	1109 kg/m (Primary age)
2.	Skin Density of Non-smokers	168 kg/m2 (Adult)
3.	Skin Density of Smokers	158 kg/m2 (Adult)
4.	Index of refraction	1.39 to 1.47
5.	Young's modulus	8.5e+06 Pa
6.	Poisson's ratio	0.48
7.	Bulk modulus /Shear modulus	7.083e+07/2.8716e+06 Pa
8.	Wavelength of absorption	500-600 nm
9.	coefficients of stiffness	0.113 /0.252 p11 p12
10.	Pockels coefficient	0.22

We use modal analysis tool box to realize this step. A new material called human skin has been created in engineering data sources of materials. Parameters of the human skin are skin density, Young's modulus, Poisson's ratio, Bulk and shear modulus. The values chosen are as documented in Table 3.Parameters indicated in the Table 2 were also used in the material parametric identification. Two types of materials like skin 2 and skin 3 are created and used to differentiate between the human skins of smokers and non-smokers respectively. Human skin density of smokers and non-smokers are 158 kg/m2 and 168kg/m2 respectively. Finite element analysis (FEA) is applied and executed on models. The first step is to have fixed support affixed at one skin face. Next with geometry and solid icon we did assignment of material. By default the assignment was structural steel. But as we need the human skin hence we chose that assignment for our simulation. We assign skin2 to smoker's class and skin3 for non-smoker's class in our simulation study [12]. Human skin models can be synthesized on system design modeler. We use sketching and extrude commands to generate a human skin model. The length and breadth of human skin are chosen to be 70 and 180 mm respectively. This model so generated is to be ported on ANSYS mechanical. The analysis settings are activated and then a face on human skin model is chosen as fixed support which is exactly opposite to the direction of the force to be applied further in harmonic analysis module. Mesh was generated using tool sets. The mesh so generated can be reduced to small size. Lesser is the size more will be accuracy of results. A command called adaptive meshing is used to generate such a size of the mesh where further reduction in size may not be possible at all for getting simulation outputs. To illustrate further steps Figures 2and 3 are references, Figure 2 depicts meshing structure and Figure 3 indicates the modal results respectively in four tabs. The Performance parameters happen to be the directional deformation at a set of harmonic frequencies. Number of modes to be generated is with the control of user commands. In the simulation run 8 modal frequencies are chosen. Number of intervals in the frequency range is also under user commands. Obtained range of frequencies for smokers class in modal analysis lies in the range of 29.735 Hz to 423.71 Hz whereas, for the non-smokers class in modal analysis lies in the range of 28.837 Hz to 410.8 Hz. Here in the modal analysis neither force nor stress can be applied to the model developed as we need to investigate the natural frequencies of vibration of the model developed.

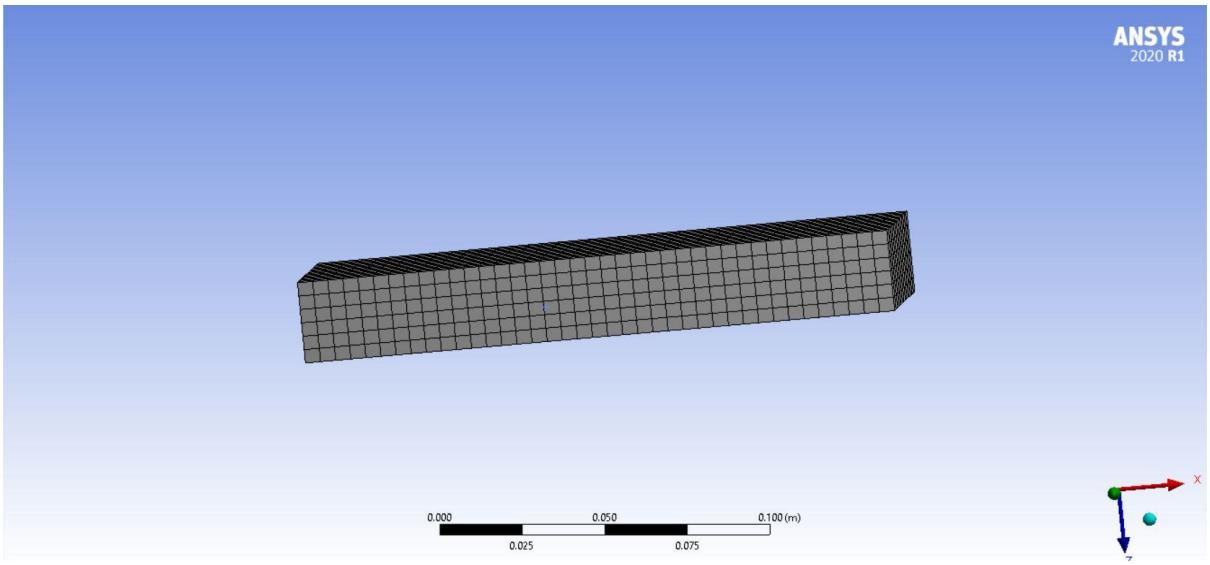

Figure.2. Mesh development stage on Human skin model for adaptive meshing of size 6.2833e-003

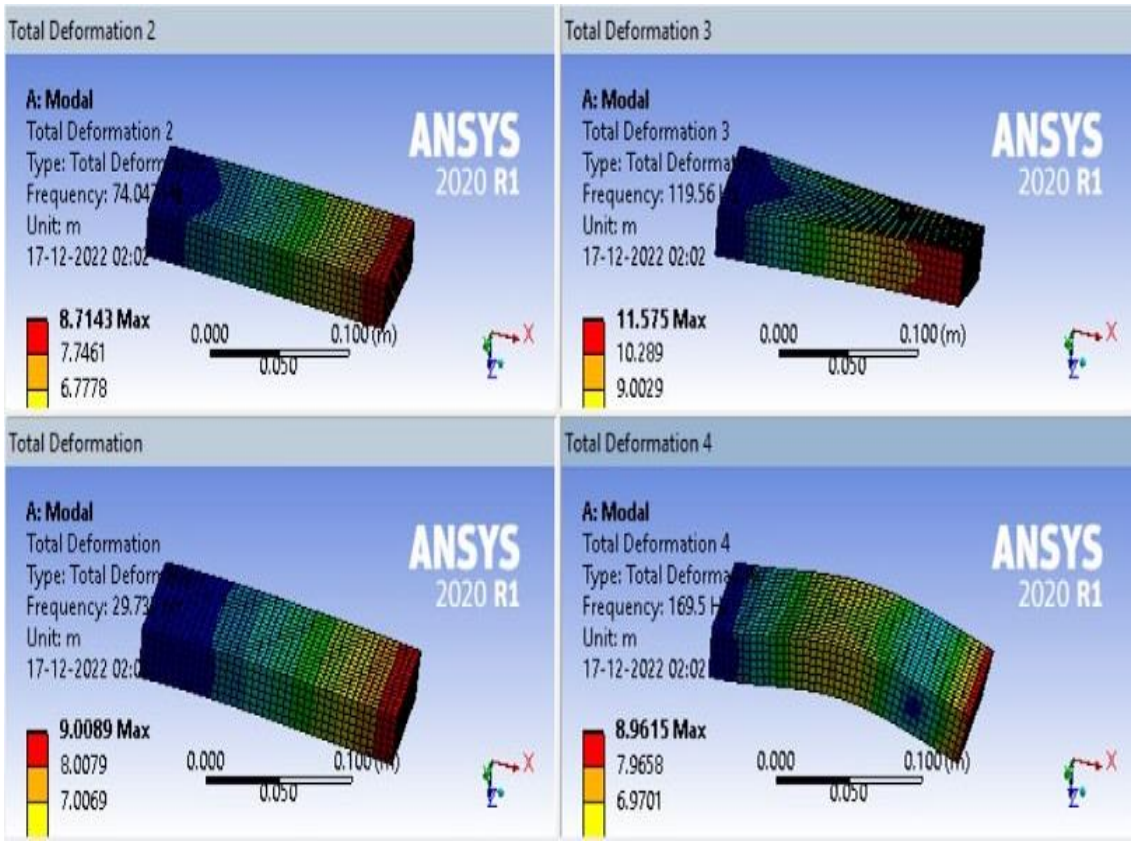

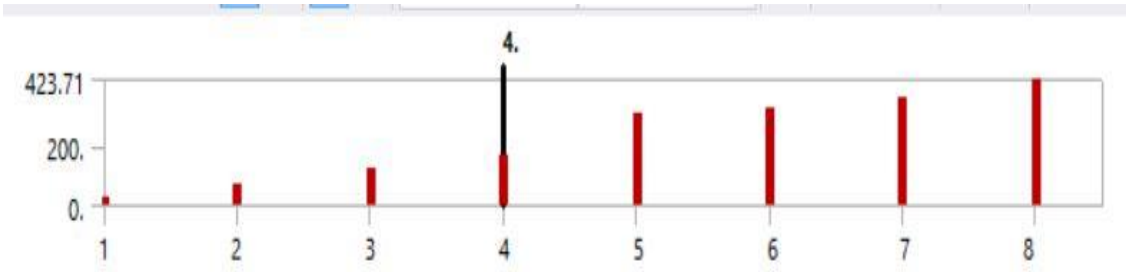

Tabular Data

	Mode	Frequency [Hz]
1	1.	29.735
2	2.	74.047
3	3.	119.56
4	4.	169.5
5	5.	307.66
6	6.	328.11
7	7.	365.29
8	8.	423.71

Figure.3. Modal simulation results on Human skin model for frequencies 29.735Hz, 74.047Hz, 119.36 Hz and 169.5Hz of modal frequencies in the four port view of ANSYS (smokers class)

C. PROCEDURE SIMULATION EXECUTION OF HARMONIC ANALYSIS

Harmonic analysis is used as a frequency analysis tool to study the model behaviours and sensitivity of model to a particular frequency and study the participation ratio of the mass among three axes. Figures 4 indicates result GUI tabs recorded in the workbench resulting from harmonic analysis. Further the output of modal analysis acts like an input to the harmonic analysis. Since already meshing and selection of assignment of material is already done, there is no need to

do these activities. Nevertheless, force will have to applied in x direction. The Force selected at beginning was 100N. In the simulation runs forces ranges from 100N to 600N and the results have been tabulated for ranges of forces. Results of the harmonic analysis of both smokers and non-smokers class have been tabulated in the section 3.1. Also in addition to directional deformation, total stress and frequency response analysis of the human skin model were recorded from simulation runs and have been captured in the study. Results obtained from deformation are discussed in section 3.1 both for smoker and non-smoker classes. As per the simulation results the range of harmonic frequencies obtained for smokers class was 8Hz to 50 Hz whereas, for the non-smokers class the frequencies ranges are from 10.625 Hz to 50 Hz. Incidentally these are the frequencies ranges where the tremors are generated in the presence of the neurological disorders. Intentionally these frequency ranges are the focuses of the study as the objective of the study is to inspect the frequencies of tremor and further to correlate these values for a presence of particular neurological disorder.

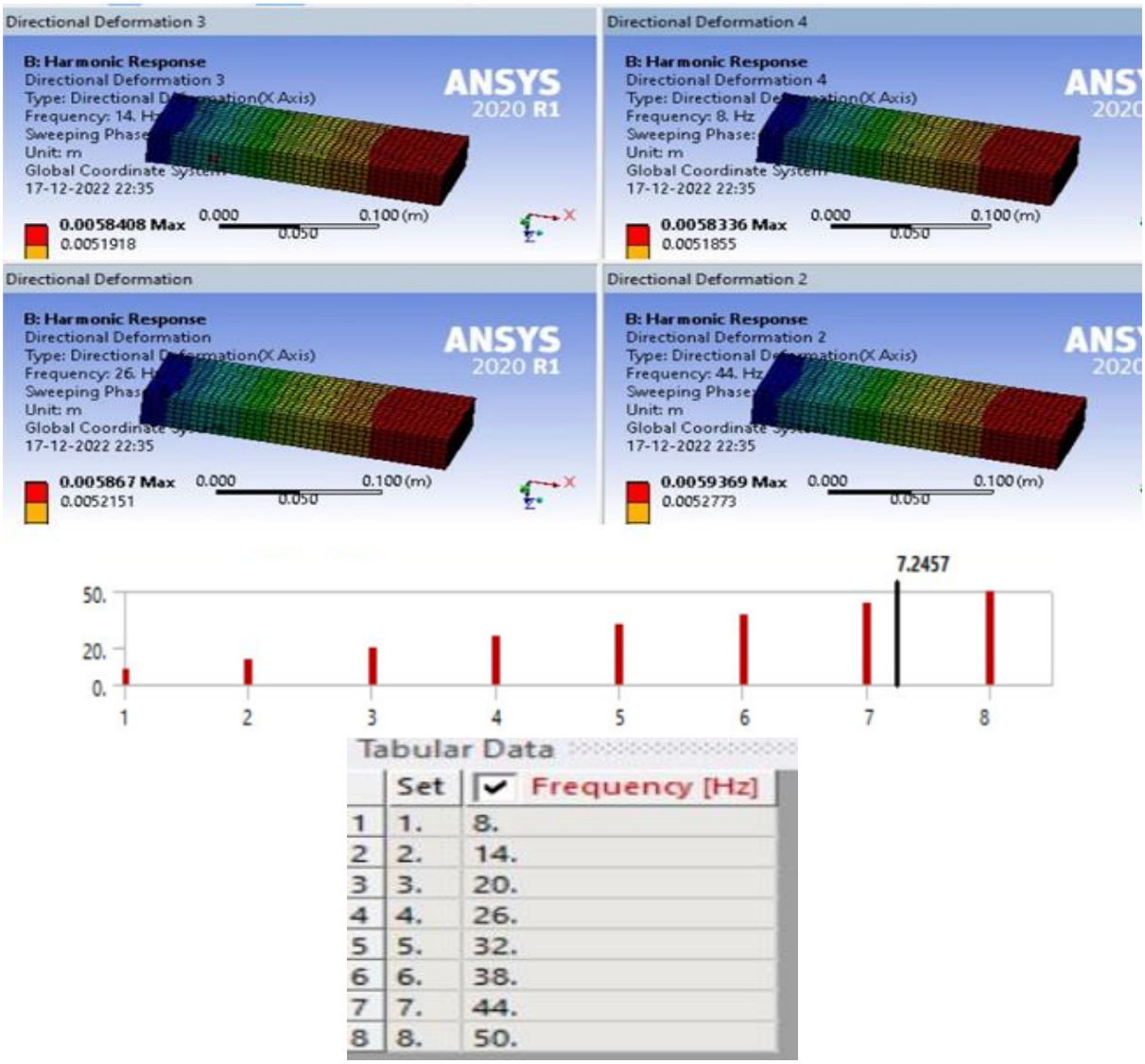

Figure.4. Harmonic analysis results on human skin model for frequencies and 8Hz, 14Hz, 26Hz and 44Hz for force applied as 600N as a four port view (smokers class)

C SIMULATION PROCEDURE IN RSOFT WORKBENCH

As per the study visualized, Deformation/tremor resulting from changes done in value of forces applied and simulations runs for various harmonic frequencies happens to be inputs to Grating Mod tool where FBG sensors are synthesized. The ranges of harmonic frequencies recorded are already indicated in the section 2.1 for both of the smokers and non-smokers class. To realize the steps 4 and 5 of method visualized we have supply deformation results as input to R Soft workbench. In order to achieve this one needs to analyse the mathematical model of Fiber Bragg grating sensor. In several literatures [21][22] the mathematical models have been discussed and have been implemented in software tools. In this study only that part of mathematical model which helps us to understand the strategy of connecting deformation values to the input of Bragg Mod tool in RSoft workbench is discussed. Though Fiber Bragg grating sensors have been implemented in software environments namely MATLAB and Python these software environments are not be suitable for studies on the FBG. It is because these softwares lack ability to work on various designs of FBG sensors like chirped FBG design, Tilted FBG design and other related designs. Optical toolboxes such as Rsoft, Lumerical are the popular

toolboxes which are suitable for such research analysis. Hence in this study Rsoft tool box has been chosen for the study undertaken.

A MATHEMATICAL MODEL OF FBG SENSOR

In the simulation study we use Bragg mod tool available in Rsoft optical workbench. The theoretical and mathematical aspects which have been used in Bragg mod tool to simulate the FBG sensor are discussed in this section. As shown the figure 5 there is Bragg grating implanted in the optical fibre in the core area. There is index modulation implanted by interference pattern of Ultra violet rays. In the interference pattern where there is constructive interference the refractive index is more and where there is destructive interference the refractive index is less. There is presence of parameter Grating Period Λ_B which varies in accordance with the external deformation and stress applied on the sensor. Due to that reason the Bragg wavelength λB varies. Mathematical relation of this variation is as indicated in the equation 5. The Bragg Condition is realized because of dual requirements: There is Conservation of energy where frequency of reflected and incident radiation is similar. In addition Conservation of momentum is present where Sum of grating wave vector and incident wave vector equal the wave vector of the scattered radiation. $K + k_i = k_f$

The Bragg Condition is represented as:

$$\lambda_B = 2\Lambda_B n_{eff} \quad (5)$$

When light of broad wavelengths enters grating only that wavelength called as Bragg wavelength λ_B gets reflected and others transmit through grating. λ_B is a function of the periodicity of grating Λ and Effective index n_{eff}[23,24].

These are the parameters which control the design of grating

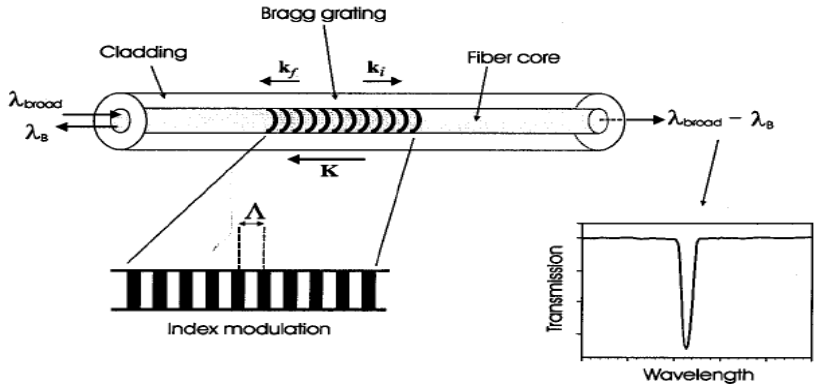

Figure5. Mathematical model of Fiber Bragg grating[23,24]

B SIMULATION STEPS IN RSOFT TOOL BOX

We use standard design of Bragg wavelength, Length, breadth, free space wavelength, core index and normalized index difference in the grating structure created in the simulation workbench of Bragg Mod tool of Rsoft workbench. After creating the taper of Bragg grating, we can administer the input simulation parameters in the Bragg grating created. In one of the pop window during simulation one need to enact on proper initializations of putting a new symbol called as Period which should be equal to 0.5264.In ending index the value of index difference should be equal to delta*1.1 (to indicate the 10% change in the difference) and also one needs to create new taper of grating by enacting on new user taper and other related commands.

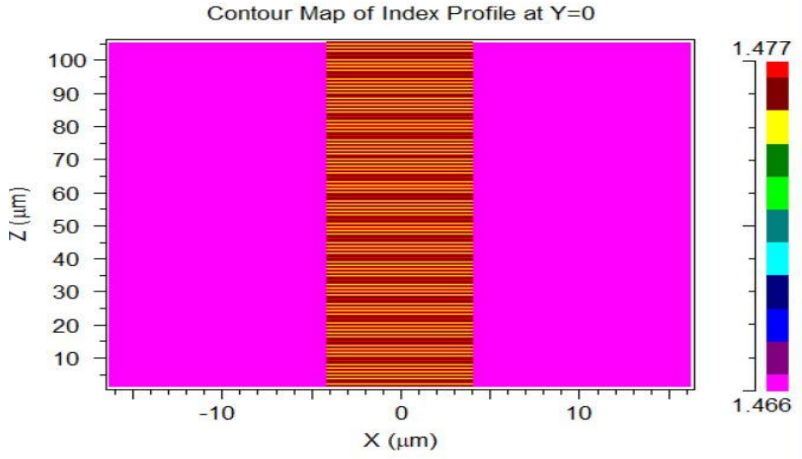

Figure6. Contour map generated of grating of refractive index ranging from 1.466 to 1.477 and period with 16 equal horizontal partitions.

In the next window in z axis the grid size and slice grid values should be initialized to one by sixteenth value of Period. Then as indicated in figure 6 a contour map of the FBG will be generated. Here as we observe the grating is indicating change in refractive index ranging from 1.466 to 1.477. There are 16 horizontal lines in the contour map indicating that the period has been divided into 16 equal partitions as per initializations done.

Following this procedure when simulation window is opened and when the grating analysis is popped up and after spectral characteristics are clicked one gets reflected spectrum of FBG as shown in the figure7.

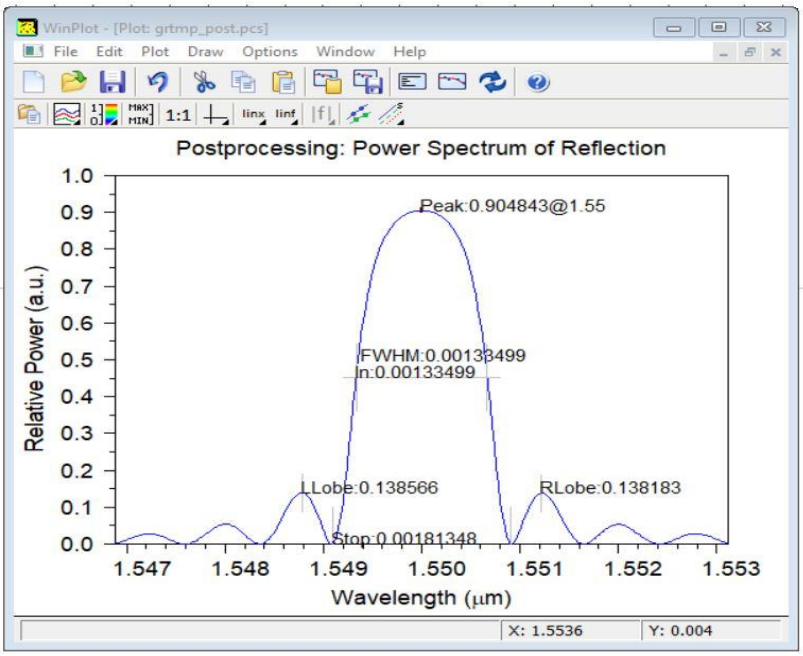

Figure7. Intializations of grating analysis and reflected spectrum of FBG at wavelength λ_B=1550nm Obtained on Rsoft tool

III RESULTS AND ANALYSIS

Results are recorded in two stages. One of the outputs is which is obtained from ANSYS workbench and their related performance parameters. The output from the ANSYS is given as input to RSoft optical test bench, we record test output results. These results are detailed in subsection 3.2. Further in subsections 3.3 inferences drawn from the results are being discussed for smokers and nonsmokers classes.

A RESULTS AND PERFORMANCE MEASURES IN ANSYS MODAL AND HARMONIC ANALYSIS

Ansys workbench modal analysis and harmonic analysis renders output results in terms of the ranges of frequencies for smokers and non-smokers classes. As highlighted in the previous section the range of harmonic frequencies for smokers class was 8Hz to 50 Hz whereas, for the non-smokers class they are from 10.625 Hz to 50 Hz resulting from simulation runs. This study is to not only contrast between the results of these frequencies but also to compare and contrast the results recorded from RSoft workbench in Bragg Mod tool. This output will be of interest to research community in the sense that it enables to differentiate the smokers class and non-smokers class from the perspective of optical sensing .Though in many of previous works done as discussed in literature review have been implemented with pure electronic sensing, in the perspective of optical sensing very limited works are being undertaken. Force will have to be applied in x direction in ANSYS workbench on the human skin model for both the classes. The Force selected at first step was 100N. In the simulation epochs range of forces is from 100N to 600N and the results of deformation obtained are tabulated for ranges of forces for each of the classes. These results have been plotted graphically for the analysis purposes in Figure 8(a) (b) and (c) for smoker's class. Though the results are documented for all the ranges of harmonic frequencies only for three critical frequencies of 8Hz,20 Hz and 32 Hz the results have been plotted .Here differences in the directional deformation values are plotted one each for 2 sets of Absolute differences in deformation at frequencies considered.

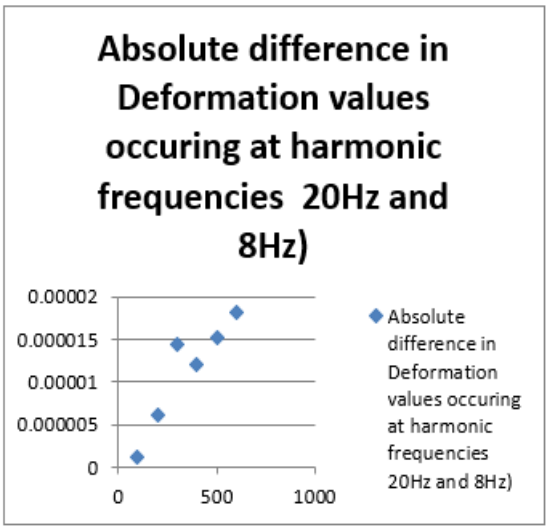

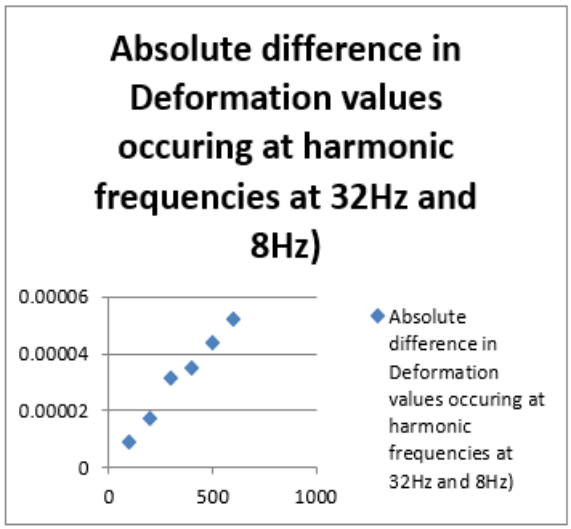

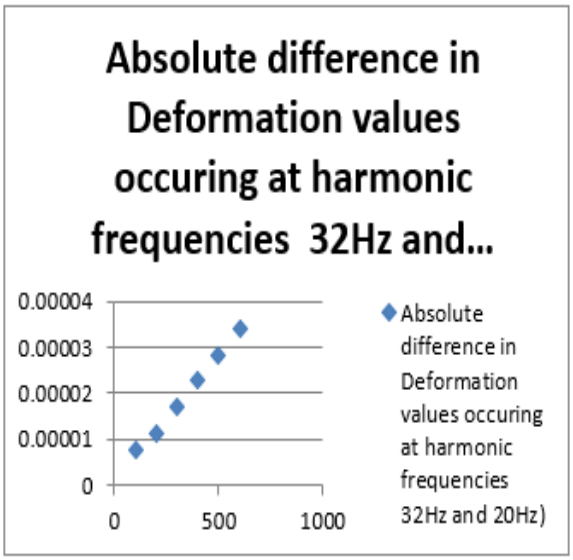

Figure 8(a)Absolute Deformation difference values at 20Hz and 8Hz Figure 8(b)Absolute Deformation difference values at 32Hz and 8Hz Figure 8(c)Aaabsolute Deformation difference values at 32 Hz and 20Hz (Smokers class) .These absolute differences in deformation values FBG sensors have picked up and changes in reflected wavelength were observed

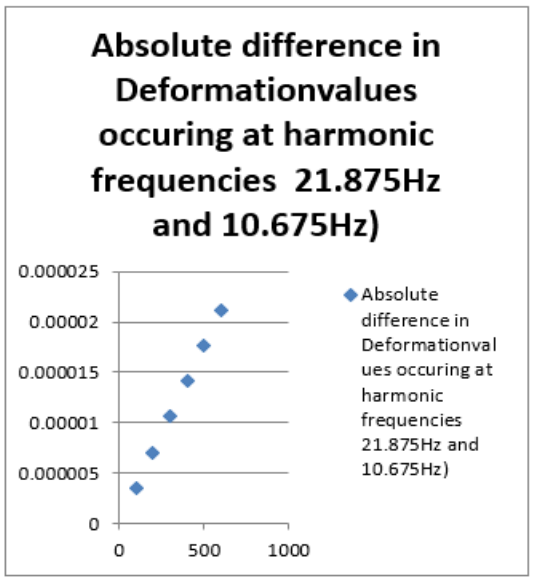

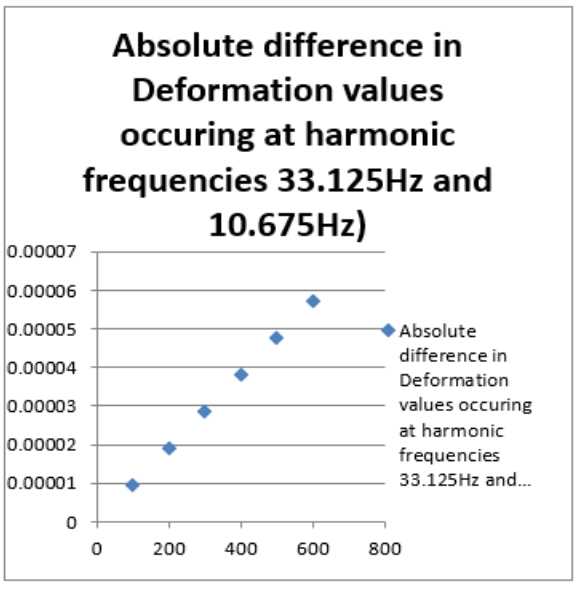

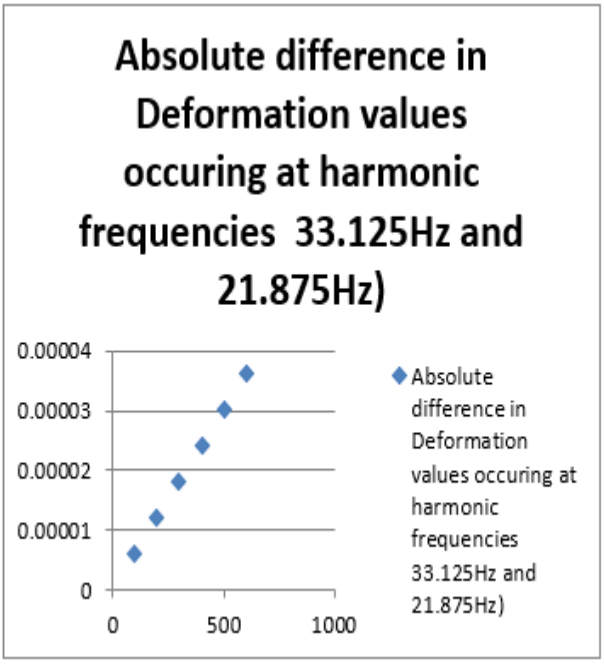

Figure 9(a) Absolute Deformation difference values at 21.875 Hz and 10.625Hz Figure 9(b)Absolute Deformation values at 33.125Hz and 10.675 Figure 9(c) Absolute Deformation values at 33.125 Hz and 21.875Hz(Non-Smokers class). These absolute differences in deformation values FBG sensors have picked up and changes in reflected wavelength were observed

As a next step forces were applied for non-smoker's class of skin models in the same ranges as that of smoker' class and their respective deformation values have been documented. Though the results are documented for all the ranges of harmonic frequencies only for three critical frequencies of 10.625Hz, 21.875 Hz and 33.125 Hz the results have been plotted. These are indicated in figures 9 (a) (b) and (c) respectively. Here differences in the directional deformation values are plotted one each for 2 sets of differences in deformation at frequencies considered. Observations here are that there are changes in the values of differences in the deformation for smoker class from that of non-smokers class. We can visualize that the difference in deformation in frequencies of 20Hz and 8Hz in smokers' class has a range well below 0.00002 where as for non-smokers class it has range above 0.00002 in the range of 21.875 and 10.675as an example. These very small differences in the frequencies optical sensor which is deployed in the study is sensitive enough and changes of reflected wavelength can be observed from the output of RSoft tool

***** PARTICIPATION FACTOR CALCULATION ***** X DIRECTION

MODE	FREQUENCY	PERIOD	PARTIC.FACTOR	RATIO	EFFECTIVE MASS	CUMULATIVE MASS FRACTION	RATIO EFF.MASS TO TOTAL MASS
1	29.7355	0.33630E-01	0.0000	0.000000	0.00000	0.00000	0.00000
2	74.0466	0.13505E-01	0.0000	0.000000	0.00000	0.00000	0.00000
3	119.557	0.83642E-02	0.0000	0.000000	0.00000	0.00000	0.00000
4	169.501	0.58997E-02	0.0000	0.000000	0.00000	0.00000	0.00000
5	307.657	0.32504E-02	0.0000	0.000000	0.00000	0.00000	0.00000
6	328.109	0.30478E-02	0.19796	1.000000	0.391897E-01	1.00000	0.787415
7	365.294	0.27375E-02	0.0000	0.000000	0.00000	1.00000	0.00000
8	423.707	0.23601E-02	0.0000	0.000000	0.00000	1.00000	0.00000
sum					0.391897E-01		0.787415

***** PARTICIPATION FACTOR CALCULATION ***** Y DIRECTION

MODE	FREQUENCY	PERIOD	PARTIC.FACTOR	RATIO	EFFECTIVE MASS	CUMULATIVE MASS FRACTION	RATIO EFF.MASS TO TOTAL MASS
1	29.7355	0.33630E-01	0.0000	0.000000	0.00000	0.00000	0.00000
2	74.0466	0.13505E-01	0.17524	1.000000	0.307094E-01	0.731381	0.617027
3	119.557	0.83642E-02	0.0000	0.000000	0.00000	0.731381	0.00000
4	169.501	0.58997E-02	0.0000	0.000000	0.00000	0.731381	0.00000
5	307.657	0.32504E-02	-0.10620	0.606034	0.112789E-01	1.00000	0.226620
6	328.109	0.30478E-02	0.0000	0.000000	0.00000	1.00000	0.00000
7	365.294	0.27375E-02	0.0000	0.000000	0.00000	1.00000	0.00000
8	423.707	0.23601E-02	0.0000	0.000000	0.00000	1.00000	0.00000
sum					0.419883E-01		0.843646

Figure10a). Mass participation ratio for x (smoker's class)

***** PARTICIPATION FACTOR CALCULATION ***** X DIRECTION

MODE	FREQUENCY	PERIOD	PARTIC.FACTOR	RATIO	EFFECTIVE MASS	CUMULATIVE MASS FRACTION	RATIO EFF.MASS TO TOTAL MASS
1	28.8369	0.34678E-01	0.0000	0.000000	0.00000	0.00000	0.00000
2	71.8091	0.13926E-01	0.0000	0.000000	0.00000	0.00000	0.00000
3	115.944	0.86249E-02	0.0000	0.000000	0.00000	0.00000	0.00000
4	164.379	0.60835E-02	0.0000	0.000000	0.00000	0.00000	0.00000
5	298.360	0.33517E-02	0.0000	0.000000	0.00000	0.00000	0.00000
6	318.194	0.31427E-02	0.20413	1.000000	0.416700E-01	1.00000	0.787415
7	354.256	0.28228E-02	0.0000	0.000000	0.00000	1.00000	0.00000
8	410.903	0.24337E-02	0.0000	0.000000	0.00000	1.00000	0.00000
sum					0.416700E-01		0.787415

***** PARTICIPATION FACTOR CALCULATION ***** Y DIRECTION

MODE	FREQUENCY	PERIOD	PARTIC.FACTOR	RATIO	EFFECTIVE MASS	CUMULATIVE MASS FRACTION	RATIO EFF.MASS TO TOTAL MASS
1	28.8369	0.34678E-01	0.0000	0.000000	0.00000	0.00000	0.00000
2	71.8091	0.13926E-01	0.18070	1.000000	0.326530E-01	0.731381	0.617027
3	115.944	0.86249E-02	0.0000	0.000000	0.00000	0.731381	0.00000
4	164.379	0.60835E-02	0.0000	0.000000	0.00000	0.731381	0.00000
5	298.360	0.33517E-02	-0.10951	0.606034	0.119927E-01	1.00000	0.226620
6	318.194	0.31427E-02	0.0000	0.000000	0.00000	1.00000	0.00000
7	354.256	0.28228E-02	0.0000	0.000000	0.00000	1.00000	0.00000
8	410.903	0.24337E-02	0.0000	0.000000	0.00000	1.00000	0.00000
sum					0.446458E-01		0.843646

Figure 10b) 10 a) & b) indicates Mass participation ratio for x and y axis for modal analysis in smokers/ non-smokers class for smokers class for x direction at frequency 328.109 mode 6 value of mass participation factor is 0.19796 where as for non-smokers class x direction at frequency 318.194 mode 6 value of mass participation factor is 0.20413

It is observed that for smokers class the mass participation factor in x axis at modal frequency 328.109 Hz is 0.19796 whereas at the similar frequency of 318.194 Hz it is 0.20413.Details of participation factor are discussed in section3.3.When the values of deformation against the nodes numbers were plotted using visualization tool boxes the plot obtained is as shown in the Figure 11.It is observed that at node numbers 2500 to 4000 the deformation values are more. Details of which are discussed in section 3.3

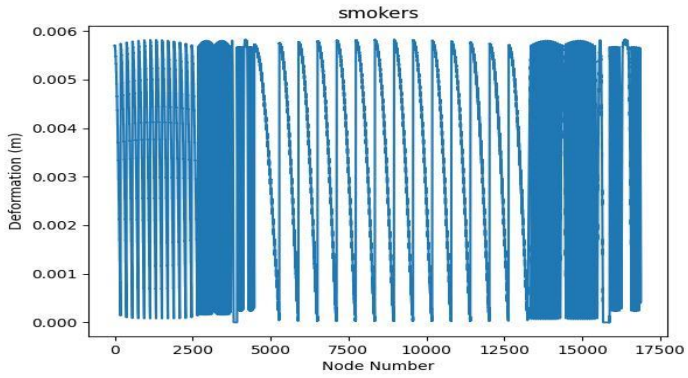

Figure11 . Visualization of deformation data for nodes in mesh in smokers and non-smokers classes deformation zones are at nodes numbered 2500 to 4000 indicating that at these node numbers failure rate of model is high

B RESULTS OF RSOFT TOOLSET

Deformation resulting on application of force has to be transformed as wavelength variations in the Fiber Bragg grating sensor. This sensor functionality can be analyzed by using Bragg Mod module available on RSoft work bench. Hence these deformation values have to converted into wavelength variations. To realize this mathematical model of the Fiber Bragg grating sensor module mathematical relationship of the Bragg wavelength is to be considered. In equation 5 this relationship is discussed given as

$$\lambda_B = 2\Lambda_B n_{eff} \qquad (5)$$

The grating reflects the light at the Bragg wavelength λ_B . λ_B is a function of the periodicity of grating Λ and Effective index n_{eff}[23,24].These are the parameters which control the design of grating

For design purpose the value of λ_B = 1550 nm and the resulting value of the periodicity of grating is to be

Calculated using equation 5

Calculating the same we get

$$\Lambda_B = \quad 1550/\,2 * 1.47 \quad = \quad 0.5264 \qquad (6)$$

If this value is used in the grating analysis of Bragg mod tool the simulated results of the Bragg wavelength should be obtained. The wavelength obtained should be 1550 nm. There are two options in the grating analysis simulation tab of software that to fix center wavelength or to fix the periodicity. Periodicity indicates the period with which the refractive index variations are happening in the Bragg grating. Reflected wavelength from grating depends on periodicity. One can vary periodicity in the grating, the effect of which is change in reflected wavelength captured in the tool box. These deformation variations will cause variations in the periodicity because they deform the grating structure.

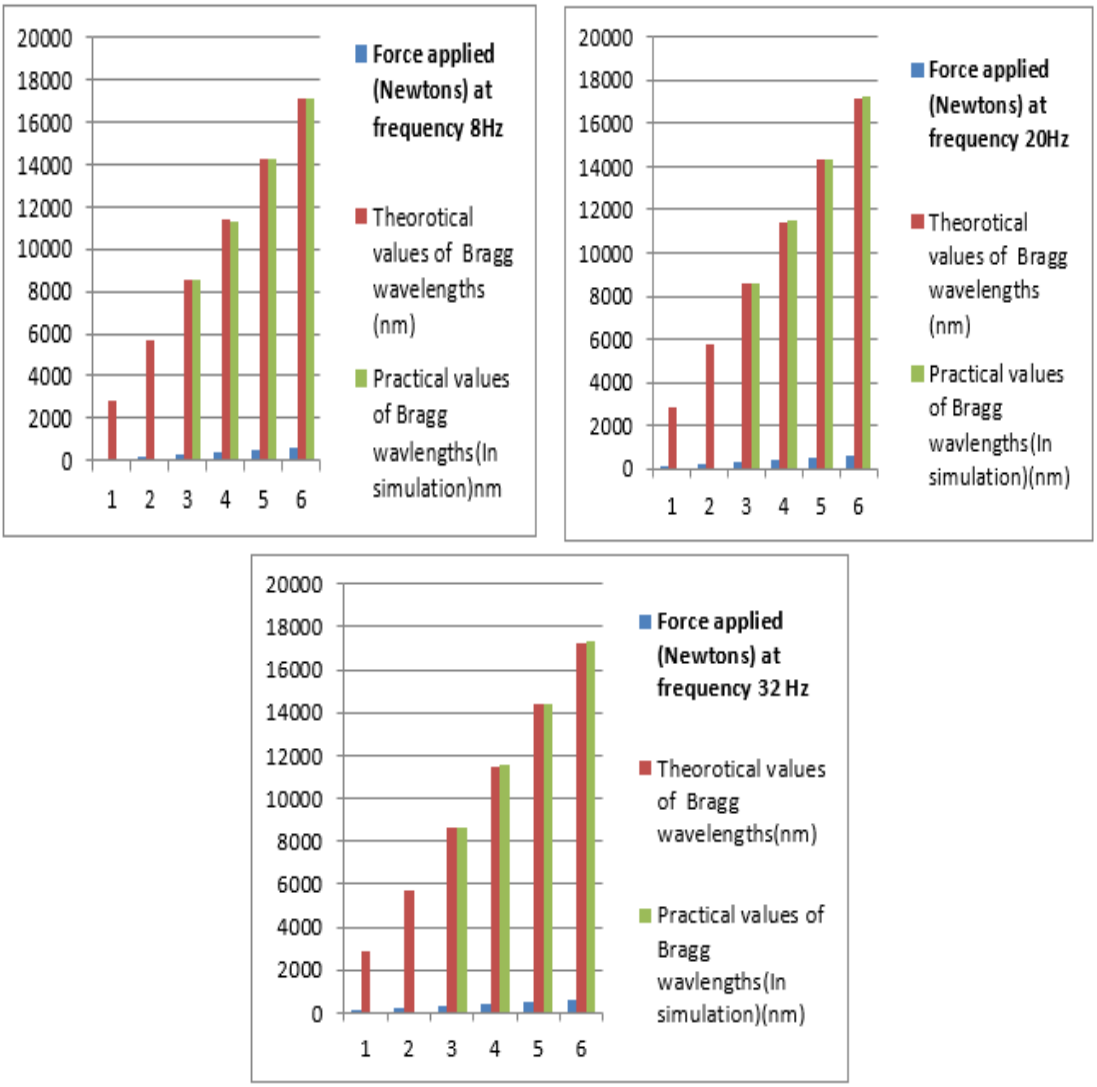

Figure 12(a) Bragg wavelength (theoretical and Practical) at 8Hz Figure 12(b) Bragg wavelength (theoretical and Practical) at 20Hz Figure 12(c) Bragg wavelength(theoretical and Practical) at 32 Hz(Smokers class)

Then both for smokers and non-smokers class these variations will be caused due to application of force. Both theoretically and practically in tool box we can visualize the variations in the changes of Bragg wavelength. These changes are plotted in for the frequencies of 8Hz, 20 Hz and 32 Hz for the smoker's class as shown in Figure 12 (a)(b) and (c). Same changes are plotted for frequencies of 10.625Hz ,21.875Hz and 33.125 Hz respectively for the non-smokers class as shown in figure 13(a)(b)(c). In both the plots theoretical and practical values obtained from tool box is plotted graphically as Bar charts. Nevertheless for Illustration purpose for a force applied 600 N for 32 Hz in smokers class and 33.125Hz in non-smokers class the reflected wavelength as obtained from Bragg mod tool is shown as in figure 14 (a) and (b) respectively. Here the shift in wavelength for smokers class for FBG sensors is 1734nm at frequency 32 Hz at force applied is 600N.The shift in wavelength for non-smokers class is 1732nm at frequency of 33.125 Hz with applied force is 600N

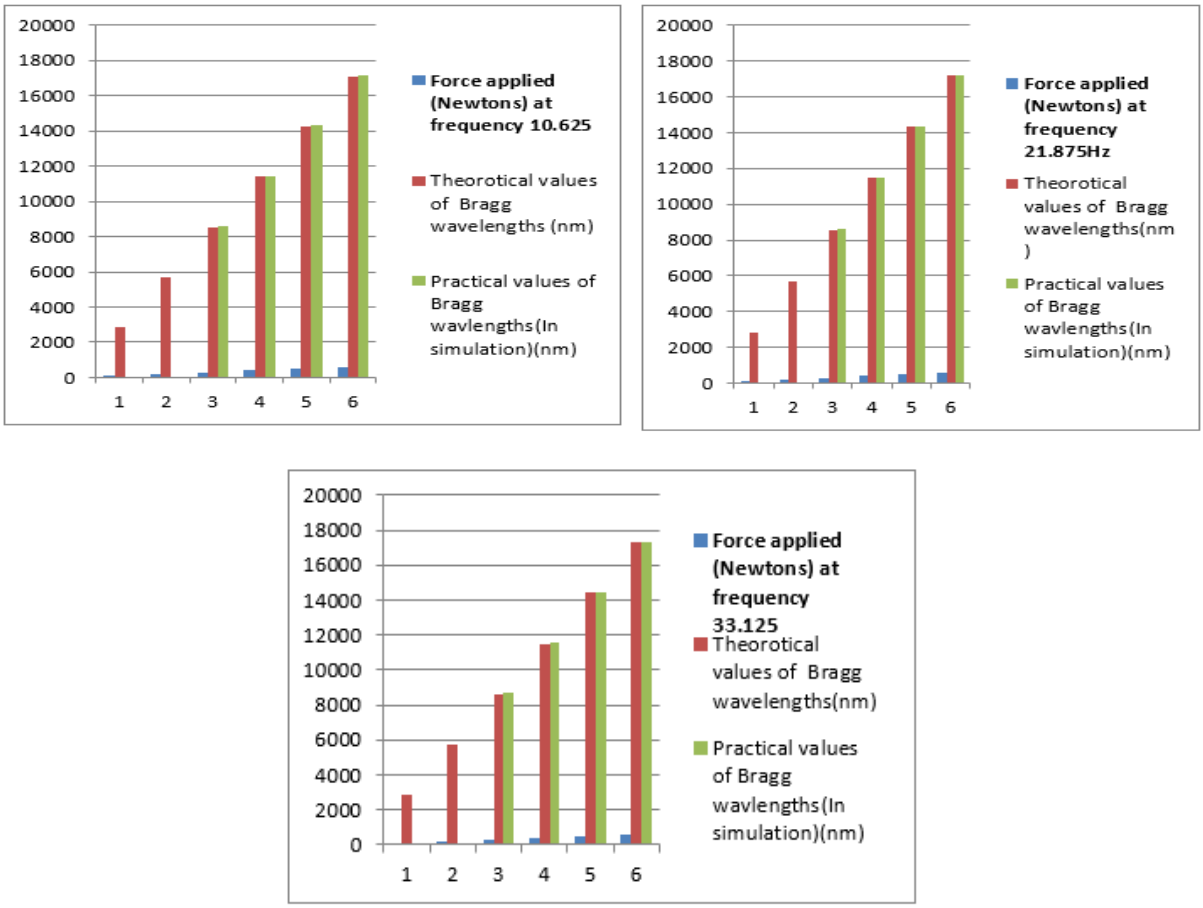

Figure 13(a) Bragg wavelength (theoretical and Practical) at 10.625Hz Figure 13(b) Bragg wavelength (theoretical and Practical) at 21.875Hz Figure 13(c) Bragg wavelength(theoretical and Practical) at 33.125 Hz (Non-Smokers class)

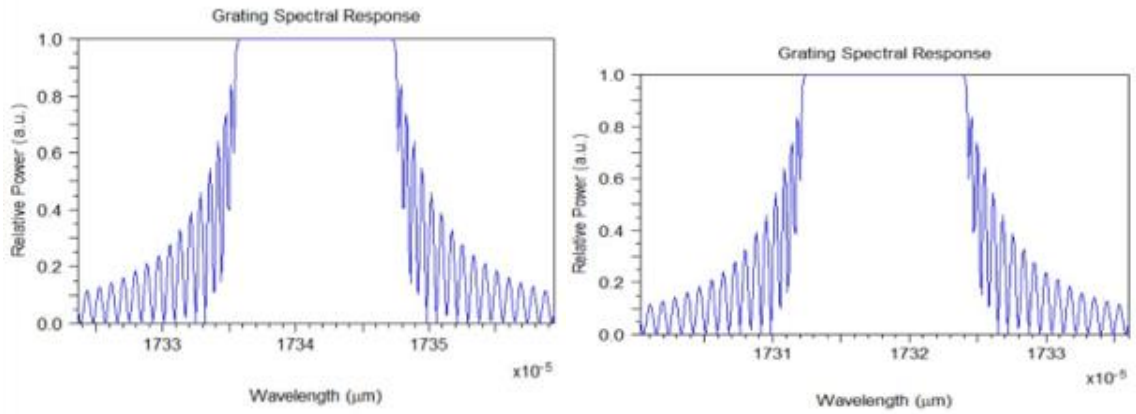

Figure 14a) Reflected spectra at 32Hz and applied force 600N for smokers class is at 17341 nm Figure 14(b) Reflected spectra at 33.125 Hz 600N for Non-Smokers class is at 17322nm as visualized.

C INFERENCES DRAWN

Observing the results we can notice that from ANSYS results perspective that there is demarcation in the values of the deformation values and mass participation ratio for both smokers and non-smokers classes. Performance parameters like the mass participation ratio is also defined for the set of modal frequencies and these parameters also have been tabulated and extracted from the analysis tool in workbench. Figure 12indicates the values for smoker's class and Figure 13 indicates those values for non-smokers class .It is observed that for smokers class the mass participation factor in x axis at modal frequency 328.109 Hz is 0.19796 whereas at the similar frequency of 318.194 Hz it is 0.20413 .There are changes in the modal frequencies which are contrasting for smokers and non-smokers classes indicating that one can identify the zones of frequencies of tremors where the human skin resonates differently for each class. Though these of some frequencies are outside the range of tremor frequencies these results will prove their utility in other related diagnostics concerning to human skin health. Yet another parameter of visualization are the deformation values which are plotted for smokers and non-smokers class. In Figure 8 a) b) c) and Figure 9a) b) c) differences between the frequencies of operation for smokers and non-smokers class are indicated. Here differences in the directional

deformation values are plotted one each for 2 sets of differences in deformation at frequencies considered. Observations here are that there are changes in the values of differences in the deformation for smoker class from that of non-smokers class. We can visualize that the difference in deformation in frequencies of 20Hz and 8Hz in smokers' class has a range well below 0.00002 where as for non-smokers class it has range above 0.00002 in the range of 21.875 and 10.675as an example. Also number of nodes and deformation values are plotted in Figure 11for visualization of deformation data across nodes. Mesh is indicated on x axis and y axis indicates deformation values at respective nodes. We can see that at mesh numbers 2500 to 4000 there are dense deformation values indicating that the probability of failure is more in that region and designers should be careful about those regions of design. Though the plots are for single set of frequencies, for all modal frequencies the results have been visualized and documented in the study.

From the perspective of the Fiber Bragg grating sensor output of reflected wavelength spectrum reflected Bragg wavelength differs for the frequencies of 8Hz, 20Hz and 32 Hz for the smokers class and for the frequencies of 10.125 Hz , 21.875Hz and 33.125 Hz for non-smokers class. Both theoretical and simulation obtained wavelengths from software tool differ for smokers and non-smokers classes. As observed in the Figures 14 (a) and (b) reflected wavelength peak is 17342 nm for smokers class and 17320 nm for non-smokers class from which we can clearly classify the smokers and non-smokers tremor regions with this subtle changes in the wavelengths visualized. We can infer from this study that method and materials practically implemented can successfully identify the tremor regions synthesized on human skin for smokers and non-smokers classes.

IV CONCLUSION

A case study to identify and classify tremors of Tobacco smokers and non-smokers tremors with the help of ANSYS and RSoft tool boxes from optical sensing perspective has been successfully implemented. The method, materials and techniques deployed in this study is classify accurately the smokers and non-smokers tremor regions. Modal analysis and harmonic analysis of ANSYS implementation in the tremor zone of frequencies of human skin is intentional as the literatures convey the fact that the tremor originates in the same zones of frequencies. This method will be a useful tool for medical diagnostics of tremor and will intuitively indicate to the doctors not only tremor frequencies but also the reasons of origin of tremors due to tobacco consumption among patients population. This study can also be extended to alcohol consumption patients and also to study of impact of aging on tremor signals. Though many studies have been conducted on electronic sensors, in the perspective of optical sensors especially of Fiber Bragg grating sensor very few studies have been undertaken. In that viewpoint this study is innovative. Future directions of this work are experimentation work with realistic sensors and deployment of multiple sensors and simultaneous extraction of tremor signals using WDM technique. Results obtained from electronic sensors have limitations in terms of noise and sensitivity and can be treated as benchmark for this study. The work done in this paper has the potential to hopefully allow researchers to design and test multiple technology platforms in a simulation environment before going into actual clinical studies.

ACKNOWLEDGEMENTS

Authors wish to acknowledge M.S.Ramaiah Institute of technology Bangalore for providing facilities to conduct this study. Authors acknowledge support of Fiber Optic technologies, Mumbai for their support on optical sensing technologies. The work done by the second author has been funded by BIRAC BT/AIR0945/PACE-19/19.

CONTRIBUTIONS FROM AUTHORS

Author 1 has theorized the concept.Author1 also has performed the simulation runs and has documented the results. Author2 has given his support on the documentation part of the work. Both authors have contributed towards the results of the paper and also discussed on the results obtained in simulation runs

CONFLICTS OF INTEREST

We hereby declare that there is no conflict of interest, conflicts of interest and other potentially conflicting interests, including specific financial interests and relationships and affiliations relevant to publication (eg, employment/affiliation, grants or funding, consultancies, honoraria, stock ownership or stock options, expert testimony, royalties, or patents filed, received, or pending).

REFERENCES:

1. Nervous system diseases Neurologic disease, December9 2020 Retrieved February 28 2021 from https://medlineplusgov/ neurologicdiseases.html
2. Tremor-Wikipedia [available online] Last updated 30th October 2022, Retrieved on 1st November 2022 from https:// en.wikipedia.Org/wiki/ Tremor.
3. Fahn S, Tolosa E, Maris C. Clinical rating scale for tremor. In: Jancovic J, Tolosa E, editors. Parkinson's disease and movement disorders. 2nd ed. Baltimore, MD: Williams and Wilkins,pp(225-234) 1993.
4. Elbe R, Comella C, Fahn S, Hallet M, Jankovic J, Juncos JL *et al*. Reliability of a new scale Essential tremor. Movement Disorders, vol(27), pp1567-69, 2012
5. Becktepe, J., Govert, F., Balint, B., Schlenstedt, C., Bhatia, K., Elble, R., & Deuschl, Exploring interrater disagreement on essential tremor using a standardized tremor elements assessment. Journal of Movement disorders clinical practice, vol(8)(3),pp(371–376),2021.
6. Grimaldi, G., & Manto, M.Neurological tremor: sensors, signal processing and emerging Applications Journal of Sensors, vol 10 (2) pp1399–1422, 2010, MDPI .

7. Lorincz, K., Kuris, B., Ayer, S. M., Patel, S., Bonato, P., & Welsh, M. Wearable wireless sensor network to assess clinical status in patients with neurological disorders In: Proceedings of the 6th international Conference on Information processing in sensor networks, pp563–564, 2007, IEEE.
8. Lee, Hong Ji & Lee, Woong Woo & Kim, Sang Kyong & Park,Hyeyoung &Jeon,Hyo Seon& Kim,Han Byul& Jeon, Beom S & Park, Kwang Suk. Tremor frequency characteristics in Parkinson's disease under resting-state and stress state conditions Journal of the neurological sciences, Vol(362),pp272–277, 2016, Elsevier
9. Roetenberg,Daniel and Luinge,Henk J and Baten,ChrisTM and Veltink,Peter H Compensation of magnetic disturbances improves inertial and magnetic sensing of human body segment orientation Journal of IEEE Transactions on neural systems and rehabilitation engineering,vol(13),(3),pp395–405,2005,IEEE.
10. Bonato, Paolo Wearable sensors/systems and their impact on biomedical engineering Journal of IEEE Engineering in Medicine and Biology Magazine, Vol22, 3, pp18–20, 2003, IEEE Publisher
11. Adewusi, S., Thomas, M., Vu, V. H., & Li, Modal parameters of the human hand-arm using finite Element and operational modal analysis. Mechanics & Industry Journal of mechanics and industry , Vol 15,(6),PP(541–549),2014
12. Yazdanparast, T., Hassanzadeh, H., Nasrollahi, S. A., Seyedmehdi, S. M., Jamaati, H., Naimian, A.,& Firooz, A.Cigarettes smoking and skin: a comparison study of the biophysical properties of skin in mokers and non-smokers, Journal of Tanaffos,,vol(18),(2),pp163,2019
13. Rao, Yun-Jiang. "Recent progress in applications of in-fibre Bragg grating sensors." *Optics and lasers in Engineering* 31.4 (1999): 297-324.
14. Heijmans, J. A. C., Cheng, L. K., & Wieringa, F. P. Optical fiber sensors for medical applications Practical engineering considerations.In:4th European Conference of the International Federation for Medical and Biological Engineering,PP2330–2334Springer, Berlin, Heidelberg.,2009.
15. Elble, RodgerJ Neuro-geriatrics Springer, pp(311—326), 2017
16. Steven J. Frucht Evaluation of patients with tremor Journal of Practical Neurology, Langone Medical Center New York 2018.
17. Online available IT'IS foundation September 29, 2000 Retrieved: from 10 March 2021 htps://itis.swiss/ virtual-population/tissue-properties/database/dielectric-properties/
18. Cormac Flynn, Andrew Taberner, Poul Nielsen, Measurement of the force–displacement response of in vivo human skin under a rich set of deformations Journal of Medical Engineering & Physics,(13)(5 PP1350–4533,2011.
19. Xiang, L., Jiang, Q., Li, Y., & Song, R. Design and experimental research on cantilever accelerometer based on FiberBragg grating Journal of Optical engineering (55)(6)PP066113,2016.
20. K.R Vidyarani, Viswanath Talasila, N Megharjun, M Supriya, K.J Ravi Prasad, G.R Prashanth An inertial sensing mechanism for measuring gait parameters and gait energy expenditure, Biomedical Signal Processing and Control Journal of Biomedical Signal Processing and control, (70)PP103056,2021.
21. Udoh, Solomon and Njuguma, James and Prabhu, Radhakrishna.Modelling and Simulation of Fiber Bragg Grating Characterization for Oil and Gas Sensing Applications. In: Proceedings of the 2014 First International Conference on Systems Informatics, Modelling and Simulation PP255-260,IEEE computer society,2014
22. Prasad, S. K., Talasila, V., & Kumar, S. Simulation and Modelling of Fiber Bragg Grating Sensors. In:2020 International Conference on Recent Trends on Electronics, Information, Communication & Technology (RTEICT) PP343-352, IEEE,2020,
23. Hill, Kenneth O and Fujii, Y and Johnson, Derwyn C and Kawasaki, Brian S Photosensitivity in optical fiber waveguides: Application to reflection filter fabrication Journal of applied physics letters(32)(10) PP647-649, American Institute of Physics,1978.
24. Meltz, Gerald and Morey, William W and Glenn, William HFormation of Bragg gratings in optical Fibers by a transverse holographic method Journal of optics letters(14)(15) PP823-825,Optical society of America,1989.